J. Braz. Chem. Soc., Vol. 23, No. 5, 880-888, 2012.
Printed in Brazil - ©2012 Sociedade Brasileira de Química
0103 - 5053 $6.00+0.00

Article

Synthesis and Thermal Behavior of New Liquid Crystals Arylaldoxime Esters

Aline Tavares,[a] Bárbara C. Arruda,[a] Elvis S. Boes,[a] Valter Stefani,[a] Hubert K. Stassen,[a] Leandra F. Campo,[a] Ivan H. Bechtold[b] and Aloir A. Merlo,[a]*

[a]*Instituto de Química, Universidade Federal do Rio Grande do Sul, Av. Bento Gonçalves, 9500, 91501-970 Porto Alegre-RS, Brazil*

[b]*Departamento de Física, Universidade Federal de Santa Catarina, 88040-900 Florianópolis-SC, Brazil*

Uma série de cristais líquidos derivados de ésteres arilaldoximas foi sintetizada e caracterizada via espectroscopia de ^{1}H, ^{13}C RMN, ATR/IV-FT e análise elementar. A estabilidade química e fotofísica desses compostos foram dependentes dos ciclos de aquecimento e resfriamento, com a decomposição sendo induzida pelo calor. As mudanças nas propriedades durante os ciclos de aquecimento foram acompanhadas através dos respectivos espectros de infravermelho. Todas as amostras se decompõem termicamente, gerando as respectivas nitrilas e ácidos carboxílicos como evidenciado pelos espectros de infravermelho e de ^{1}H NMR. As propriedades mesomórficas foram avaliadas apenas no primeiro ciclo de aquecimento, devido à decomposição térmica observada após a primeira transição para o estado isotrópico. Espectros de absorção em solventes orgânicos apresentam três bandas entre 230 e 340 nm, e uma banda de emissão, larga e sem estrutura, em 430 nm. Cálculos teóricos *ab initio* foram realizados para a obtenção de informações estruturais dos ésteres arilaldoximas.

We report the synthesis of a series of liquid-crystalline materials based on arylaldoxime esters and the characterization of these materials by ^{1}H, ^{13}C NMR, ATR/FT-IR spectroscopy and elemental analysis. The chemical stability and liquid-crystalline as well as photophysical properties of the compounds are described being dependent on the heating/cooling cycles. The changes in chemical stability and the liquid crystals properties of arylaldoxime esters were observed during these thermal cycles by IR analysis. All samples underwent a thermal degradation yielding the corresponding nitriles and carboxylic acid as evidenced by IR and ^{1}H NMR spectra. Due to the decomposition process, information about the mesomorphic behaviour is lost. The UV-Vis absorption spectra in solution display three absorption bands between 230 and 340 nm. The fluorescence spectra exhibit a broad and structureless emission band located at 430 nm. *Ab initio* calculations were performed to obtain information on the molecular structure and properties of the title compounds.

Keywords: arylaldoxime esters, liquid crystals, infra-red analysis, isoxazolines

Introduction

Carbonyl compound derivatives possessing a carbon-nitrogen double bond have been recognized as attractive synthetic targets due to their potential application in medical and material chemistry.

Schiff bases, which are the most popular class of theses carbonyl derivatives, have been reported as important materials in coordination chemistry,[1,2] analytical chemistry[3,4] and liquid crystal science.[5-12] Oximes are less popular than Schiff bases, but they are found in many practical applications.[13] For example, (*E*)- and (*Z*)-oximes were used to elucidate action mechanisms of their dehydration catalyzed by liver cytochromes P450.[14] Bisaryloxime ethers were found to be active inhibitors *in vitro* of plasma protein transthyretin (TTR) which is responsible of amyloid fibril formation.[15] Perillartine is the oxime derived from perillaldehyde, found in *Perilla frutescens* (Lamiaceae). It is known as perilla sugar being 2000 times sweeter than sucrose.[16] Pralidoxime is another example of an oxime, which is able to bind to organophosphatate-inactivated acetylcholinesterase.[17] Benzisoxazoles are present in a large number of important products

*e-mail: aloir@iq.ufrgs.br

with pharmacological properties and are synthesized by [3+2] cycloaddition reaction of a benzyne with a nitrile oxide.[18] Isatin is a natural product found in plants of *genus Isatis*. Many of its derivatives, which are used in drug synthesis are obtained from precursors derived from oximes.[19] Oxime-derived, chloro-bridged palladacycles represent very efficient catalyst precursors for the Heck olefination of haloarenes.[20] Recently, oxime carbonates were introduced as novel reagents for the instalation of Fmoc and Alloc protecting groups, free of side reactions.[21]

As part of our continuing interest in the synthesis of new liquid crystals (LC) derived from 3,5-disubstituted isoxazolines, from [3+2] 1,3-dipolar cycloaddition reaction between aryl nitrile oxide and alkene,[22] and others[23] we explored the synthetic potential of the arylaldoximes, as a precursor of aryl nitrile oxide, in the preparation of new LC materials. The initial strategy utilizes arylethynylbenzaldehyde oxime, an advanced intermediate in our research program involving the preparation of novel isoxazoline liquid crystals,[24] as a key component for the synthesis of mesogenic arylaldoxime esters.

In the present article, we report the synthesis and the physical chemical behaviour of a series of arylaldoxime esters **6a**-**d** and **8** derivatives as well as the intermediates **3** and **4**. The liquid-crystalline properties, ATR/FT-IR spectra, differential scanning calorimetry (DSC) X-ray experiments, absorption and fluorescence spectra are reported.

Experimental

Instruments, techniques, spectrum data are available in Supplementary Information. The experimental conditions were adapted from literature.[25-28]

Results and Discussion

Synthesis

Scheme 1 describes the intermediates and the final liquid crystals synthesized in this work. A two-step process was applied to synthesize the aryloxime **4**. The route begins with a Sonogashira cross-coupling reaction[29] of the terminal acetylene **1**[28] and commercial *p*-bromobenzaldehyde (**2**) in dry triethylamine. The following step produces the oxime **4** from a reaction of aldehyde **3** under mild conditions in an aqueous ethanol solution of hydroxylamine hydrochloride and sodium acetate.

The homologous series of arylaldoxime esters **6a-d** was prepared in order to investigate the effect of the benzoyl group on liquid crystals and photophysical properties. In addition, the benzoyl group linked to the oxime allows evaluating the conformational aspects related with rotamers around the N–O bond that are possible in these compounds (see the topic *Ab initio* calculations). Thus, four compounds **6a**-**d** were synthesized by esterification of oxime **4** with 4-alkoxybenzoic acids **5a**-**d**[25,28,30] using DCC/DMAP protocol.[31]

Considering our recent results using isoxazoline as molecular kits for liquid-crystalline materials[22] we are reporting also the synthesis and the LC behaviour of a single LC containing the isoxazoline ring. To compare, we selected the acid **7** as a chemical partner of the oxime **4**. The final compound **8** was then synthesized by applyng the same reaction protocol used for compounds **6a**-**d**.

Liquid-crystalline behaviour

The LC properties were investigated by polarizing optical microscopy (POM) and differential scanning

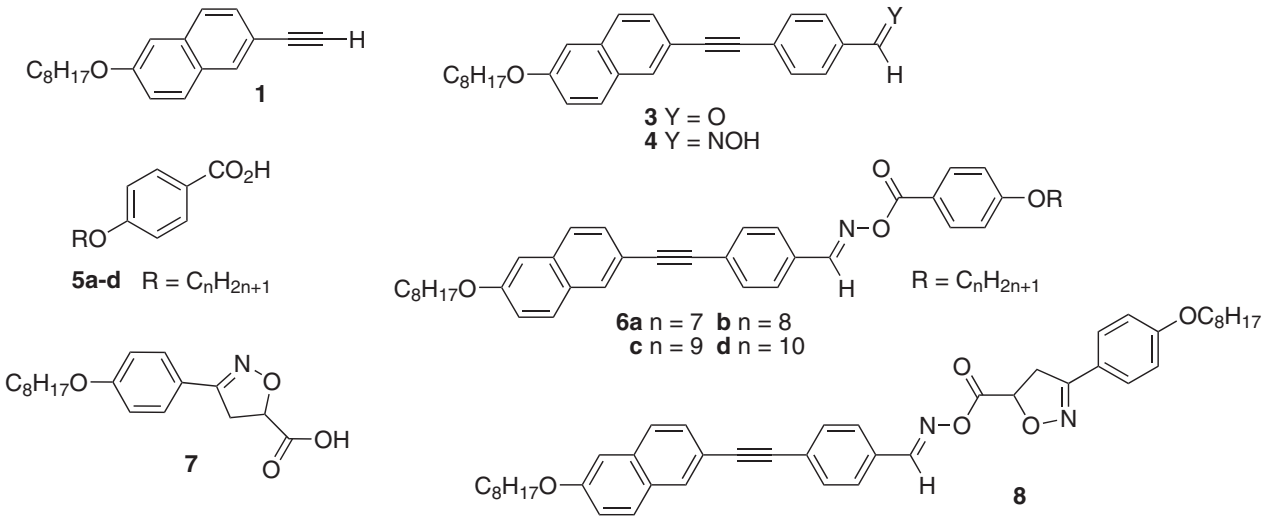

Scheme 1. The chemical intermediates and the final liquid crystals **6a-d** and **8**.

calorimetry (DSC). The transition temperatures and enthalpics of compounds **3**, **4**, **6a**-**d** and **8** are summarized in Table 1. As expected, compounds **3** and **4** exhibited the enantiotropic nematic mesophase. On cooling, **3** and **4**, showed birefringent droplets followed by large areas of planar orientation, schlieren texture which are the characteristic features of the nematic phase. The transformation of **3** into the oxime **4** indicates that the presence of the C=NOH group in substitution of C=O furnishes a stable mesophase probably due to the stronger dipole of the oxime and the possibility of association by intermolecular hydrogen bonds. This is also corroborated by the larger enthalpy of **4** for the transition of the nematic to the isotropic phase obtained from DSC traces.

Liquid-crystalline aldoximesters and ketoximesters have been published first by Weissflog *et al.*[32] They founded that some of these oximesters are unstable under heating decomposing above the clearing temperatures. Compounds **6a**-**d** and **8** synthetized in this work display similar thermal unstability when heated. Thus, when the samples were subjected to the heating/cooling cycles, the DSC profiles exhibited different behaviours. As an example, the modification of the DSC traces in the heating/cooling cycles of the samples **6c** and **8** are represented in Figure 1. The increased length-to-breadth ratio of the arylnaphthylacetylene group bonded to the oxime ester is not sufficient to maintain the thermal stability of these new LC aryloxime esters. The data in Table 1 were collected only in the first cycle due to the chemical decomposition observed above the clearing temperature. It can be seen that original LC properties of these compounds is vanished after the first heating cycle. The thermally induced degradations were more intense after the samples entered the isotropic phase during the first heating run. The DSC traces show that all samples when heated at first time presented irreversible endothermic transitions. For example, the selected peak at 155 °C, as shown in Figure 1, is associated with the transition crystal phase Cr_2 to SmC mesophase, which disappeared after the first heating. On cooling, the new and low intensity broad peak that arises around 139-143 °C which is attributed to unknown concentrations of starting oxime ester and decomposition products, probably the corresponding alkyloxybenzoic acid and the related nitrile.[32]

Table 1. Transition temperatures (°C)[a] and enthalpy values (kcal mol^{-1}, in brackets) for compounds **3**, **4**, **6a**-**d** and **8**

LC	First heating cycle T / °C (ΔH / (kcal mol^{-1}))
3	Cr 107 (5.5) N 151 (0.04) I
4	Cr 151 (4.1) N 176 (0.7) I
6a	Cr_1 96 (1.1) Cr_2 139 (4.7) SmC 153 (0.1) N 175 (0.1) I
6b	Cr_1 99 (6.3) Cr_2 133 (5.7) SmC 170 (0.06) N 173 (0.04) I
6c	Cr_1 102 (4.2) Cr_2 155 (10.1) SmC 170 (0.07) N 184 (0.2) I
6d	Cr_1 78 (0.4) Cr_2 108 (1.2) Cr_3 135 (6.2) SmC 170 (0.04) N 174 (0.1) I
8	Cr 109 (2.4) SmX[b] 146 (0.7) I

[a]Peak temperature; scan rate: 10 °C min^{-1}; Cr = crystal phase; SmX = smectic X phase, SmC = smectic C phase and N = nematic phase; [b]ref. 33.

It is almost impossible to determine the mesophase behavior after the first heating cycle. The compounds **6a**-**d** decompose thermally forming a mixture of unknown ratio composition of the nitrile and 4-*n*-alkyloxybenzoic acid. Such degradation products have already been characterized treating aldoxime esters under basic conditions.[34] The following mesophase sequence is assigned to pure nitrile **10**: Cr 95 N 157 I (DSC)[35] and acid **5a**: Cr 101 SmC 107 N 145 I,[36] respectively (see Supplementary Information

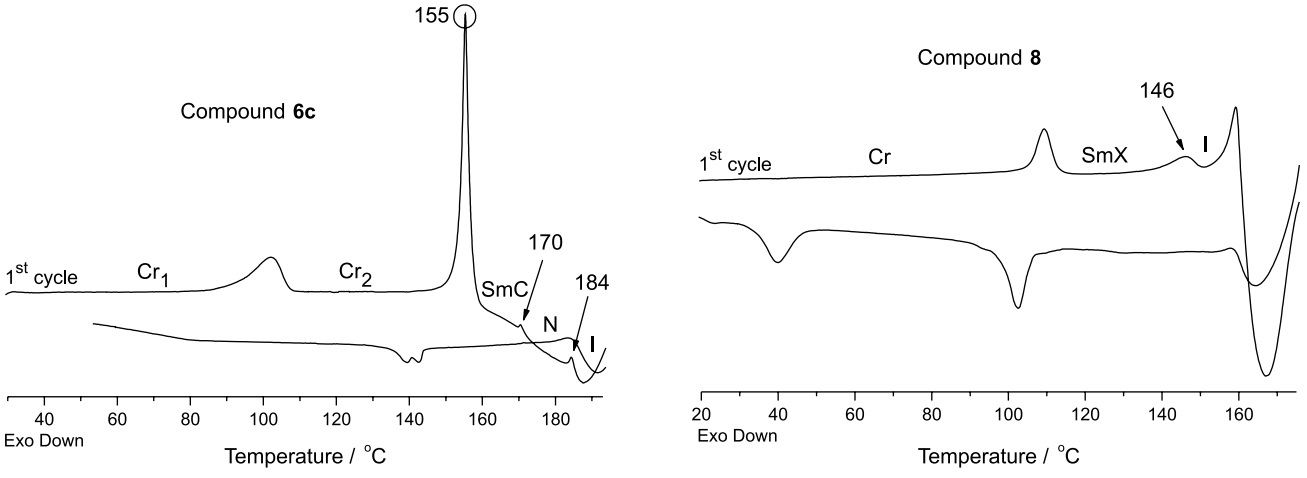

Figure 1. DSC thermograms of **6c** and **8** on 1st heating/cooling stages at rate 10 °C min^{-1}. The peak temperature is given.

for the synthesis). The degradation of these compounds was also observed in the ATR/FT-IR analysis. Figure 2 describes four ATR/FT-IR spectra of the sample **6c** under four different conditions: (a) before heating (no thermal history); (b) spectrum collected from the sample that underwent many heating/cooling cycles, (c) spectrum recorded for the sample that remained overnight at room temperature; (d) ATR/FT-IR spectrum obtained from the batches of crystals (20 mg) of **6c** that were heated at 185 °C for 15 min and cooled to room temperature. After thermal treatment, **6c** was dissolved again in $CHCl_3$ and then the solvent was evaporated. The pale yellow solid obtained was washed with ethanol and dried. In (e) the spectrum of the synthesized nitrile-LC **10** is presented.[35]

The set of the ATR/FT-IR spectrum shows clearly a change in the region of 1600-1750 cm^{-1}. In (a), **6c** displays a strong absorption at 1733 cm^{-1} which corresponds to the carbonyl group stretching. However, this absorption peak is shifted to lower frequency after heating/cooling cycles in (b) and (c) in Figure 2. The main modification is the appearance of a large peak at 1671 cm^{-1}. In (d) we can see that the **6c** does not return to the original condition. The absorption peak at 1671 cm^{-1} is accompanied by another peak at 2223 cm^{-1} which is an indication of the C≡N group resulting from the thermal decomposition. A broadening of peak at the left side in (d) is seen associated with formation of carboxylic group. The absorption band at 2207 cm^{-1} is related to the C≡C group. The peak at 1090 cm^{-1} is assigned to the N–O–C group. The N–O–C stretching vibration appears in the recorded spectrum of the first heating (a) and it is absent in the other spectra (b-d). The changes observed in the peaks at 1733 cm^{-1} and 1090 cm^{-1} clearly indicate that the decomposition is being induced continuously during the cycles of heating and cooling. The decomposition is indeed an elimination reaction induced by heat.

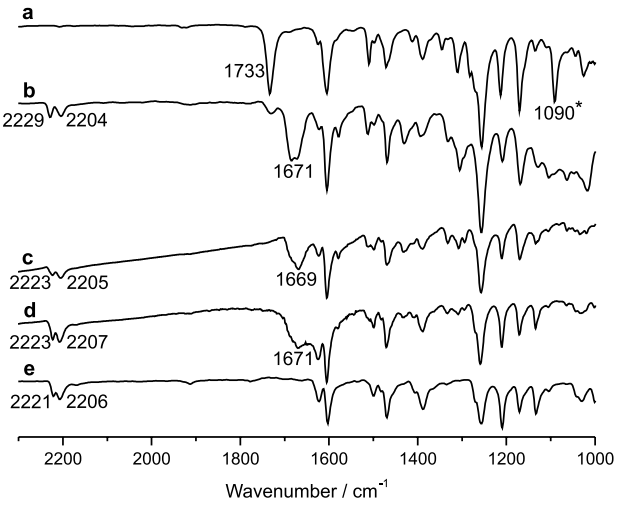

Figure 2. Portion of the ATR/FT-IR spectra: (a) original sample of compound **6c** without heating/cooling cycles; (b) spectrum obtained of **6c** after many heating/cooling cycles; (c) spectrum of the same sample **6c** in (b) after overnight at room temperature; (d) spectrum of **6c** after thermal and solvent treatment (see text for discussion); (e) compound **10**. The absorption band assigned to the N–O–C group appears at 1090 cm^{-1} in (a).

The nature of the mesophase of these esters observed during the first heating was studied and characterized by POM and X-ray diffraction. So, the sequence smectic C and nematic was observed for oxime ester **6c**. When the samples were slowly heated, the schlieren texture appeared showing singularity lines with four dark brushes in some domains. At SmC → N transition, the samples become more fluid and schlieren texture exhibit singularity lines with two and four dark brushes and homeotropic texture-dark region.[37] The mesophase identification for **8** was critical due to the decomposition of the samples when heated. We tried to determine the nature of this mesophase combining the X-ray data and POM analysis, but our attempts failed. The texture of the mesophase of **8** during the first heating is mosaic-like texture, (Figures S40 and S41 in Supplementary Information)[38] and it was named as SmX. In this sense, LC **8** present the following phase sequence taken from the first heating: crystal phase Cr → SmX → I.

The X-ray diffraction experiments were carried out with compounds **6a-d**. For compound **6a** the spectrum recorded during the first heating cycle at 150 °C in the SmC phase contain a sharp peak in the low-angle region, arising from the reflection of the X-ray beam on the smectic layers, and its corresponding second order peak (Figure 3). The inter-layer spacing was obtained by applying Bragg's law to the first maximum. The smectic order was confirmed by the ratio of the value obtained for the first peak with respect to the value obtained for the second order peak. It is well known that this ratio must obey the relation 1:1/2:1/3:1/4… in smectic phases.[38] The obtained inter-layer spacing was 37.3 ± 0.1 Å, which is shorter than the calculated molecular length considering the distances between the far atoms with the addition of the van der Waals radii from hydrogen atoms bonded to the first and last carbon atoms in the chain (at level RHF/6-311G(d,p), see discussion below). The calculated value for the fully extended all *trans*-conformation is l = 43.1 Å. The reduction of about 5.8 Å is consistent with the conformational disorder of the chains in the mesophase and due to the molecules inclination in the SmC phase.[38] This observation is consistent with the POM texture observed for **6a** on the first heating which was assigned as SmC phase. From the collected X-ray spectrum of the compound **6a** powder, before the first heating cycle, we obtained also a smectic order with a spacing layer of 39.3 ± 0.1 Å, but the additional peaks around 2θ = 20 degrees indicate a crystalline structure (Figure 3). The compounds **6b-d** presented similar behavior.

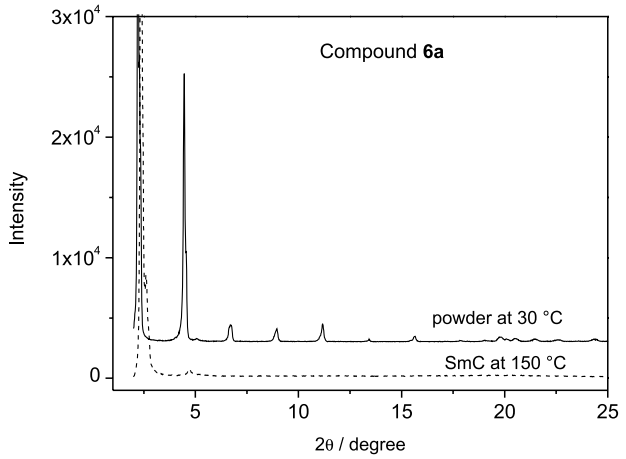

Figure 3. X-ray diffraction patterns of compound **6a**.

Ab initio calculations

Ab initio calculations were performed in order to obtain information about the molecular structure and properties such as relative energies of molecular conformations, rotations barriers, molecular dimensions and electrostatic properties. The calculations were carried out with the package Gaussian 98, Revision A.9[39] at the RHF/6-311G(d,p) level of theory. We selected the LC compounds **6a** as a representative of this study to correlate the phase behavior and structural features. We performed the geometry optimization of the molecular structure and found a structure corresponding to a point of minimum energy confirmed by the absence of imaginary frequencies in the normal mode analysis calculation. The molecular size, calculated for this optimized structure as the distance between the hydrogen atoms located at opposite ends of the alkyl chains, is 43.1 Å (Figure 4). This is the length of the largest molecular axis. In addition we have studied the barrier height for the conformers *cis* and *trans* of this molecule corresponding to the rotation of the dihedral angle C–N–O–C generated by the rotation around the N–O bond. Therefore, we have optimized the molecule with dihedral angles C–N–O–C of 0.0 and 180.0 degrees corresponding to the *cis* and *trans* conformers respectively. We have found that the *cis* conformer is not a stationary point for this structure and we have performed the geometry optimization of this conformer keeping the dihedral angle C–N–O–C fixed at an angle of zero degrees while allowing the optimization of all the other angles and bond lengths in the structure of the molecule in this conformation. In this case, we optimized the molecular structure with the molecule constrained to the *cis* conformer for the dihedral angle C–N–O–C.

Then we compared the energies calculated for the *trans* and *cis* conformers and we have found the difference of 7.4 kcal mol^{-1} (31.0 kJ mol^{-1}). This is the barrier height for the rotation of the dihedral angle C–N–O–C, corresponding to the difference in the energies calculated for the *cis* and *trans* conformer of this molecule.

The electrostatic analysis also provides us the dipole momentum for this molecule which is 4.23 D (debyes) for the *trans* conformer and 2.69 D for the *cis* conformer. The dipole vector points along the shortest molecular axis or in the direction orthogonal to the longest molecular axis. The high energy calculated for this rotational barrier prevents the rotation of the groups around the N–O bond at ordinary or room temperatures and contributes to enhance even more the structural rigidity of this molecule.

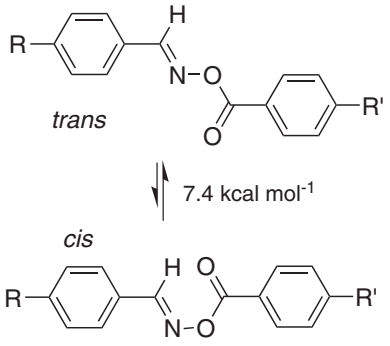

Figure 4. *Trans* and *cis* conformation for **6a** - the alkyloxy chains and naphtylacetilenic group have been omitted for clarity.

The most stable conformation obtained theoretically in this work is in agreement with previous work published by Altinbas *et al.*[40] describing the crystal structure of the *E*-benzaldehyde *O*-benzoyloxime. They found that the crystalline structure of this aromatic oxime is better described by the *trans* conformation where the C–N–O–C dihedral angle is approximately equal to 180.0 degrees.

The thermal behaviour of the series **6a-d** displayed distinct behavior to **8**. These data suggested that the non-colinearity of the two planes of the isoxazoline ring (about 135.9 degrees)[41] cause an influence on the stability of the mesophase. Due to the introduction of isoxazoline ring, the molecular symmetry is lowered changing the mesophase nature found in this work. The isoxazolinic system disfavours the interactions between the planar cores reducing the intermolecular forces responsabile for packing arrangements in the mesophase. It should be noted that the presence of the naphthalene ring induces the formation of more stable mesophase due to increased molecular interactions.[42]

Photophysical properties

The photophysical properties of compounds **3**, **4**, **6c** and **8** in dioxane, chloroform, ethanol and acetonitrile are listed

in Table 2, and their UV spectra are shown in Figure 5. The spectra of all compounds clearly exhibit the two bands of the naphthalene ring,[43] a major band at short wavelengths (220-260 nm), resulting from excitation along the major axis of the molecule (the β-band), and a two-peak band (*p*-band) between 250-300 nm. As has been observed by Marsh *et al*.,[43] the addition of a ethynyl group preserves the major features of the absorption bands of naphthalene. On the other hand, the long-wavelength band around 340 nm can be attributed to the charge-transfer transition. In fact, a third band in these systems is evidently different from the spectra of naphthalene or ethynylnaphthalene[43,44] indicating that conjugation effects of the aryl group and the ethynyl-naphthalene are pronounced.

Although the free rotation of the ethynyl group may result in a steric effect that minimizes the conjugation effect of these groups,[45] the electronic interaction between the electrons of the aryl substituents and the 2-ethynyl-6-(octyloxy)-naphthalene ring plays an important role in activating the π-conjugation.[46] Thus, we assumed that the ground-state absorption can be attributed to the local excitation of the 2-ethynyl-6-(octyloxy)naphthalene chromophore. The absorption peaks of compounds **3**, **4**, **6c** and **8**, show little dependence on the solvent polarity which implies that the solvent stabilization of the ground state species is not significant.

The fluorescence emission spectra of the compounds **3**, **4**, **6c** and **8** (Figure S44) were recorded in the same solvents (dioxane, chloroform, ethanol and acetonitrile) and in the solid-state using an excitation wavelength at 343 nm. Table 2 summarizes the emission maxima, Stokes' shift and quantum yield (ϕ) in the studied solvents and in the solid-state. The results show that all compounds emitted violet-blue light in solution and in the solid state. We observed constant emission band profiles in the 290-350 nm range of excitation wavelength. The Stokes shift observed is very small (40-98 nm) suggesting similar geometries for the S_0 and S_1 states. All the fluorescence spectra are quite similar and the peaks appear at 350-550 nm with a hypsochromic shift produced in dioxane. The λ_{em} was shifted to longer wavelength (*ca*. 40 nm) when the aldehyde is the bearing group of the aryl ring. The spectra of the compounds in solution lose the characteristic of naphthalene fluorescence emission and show a broad and structureless emission

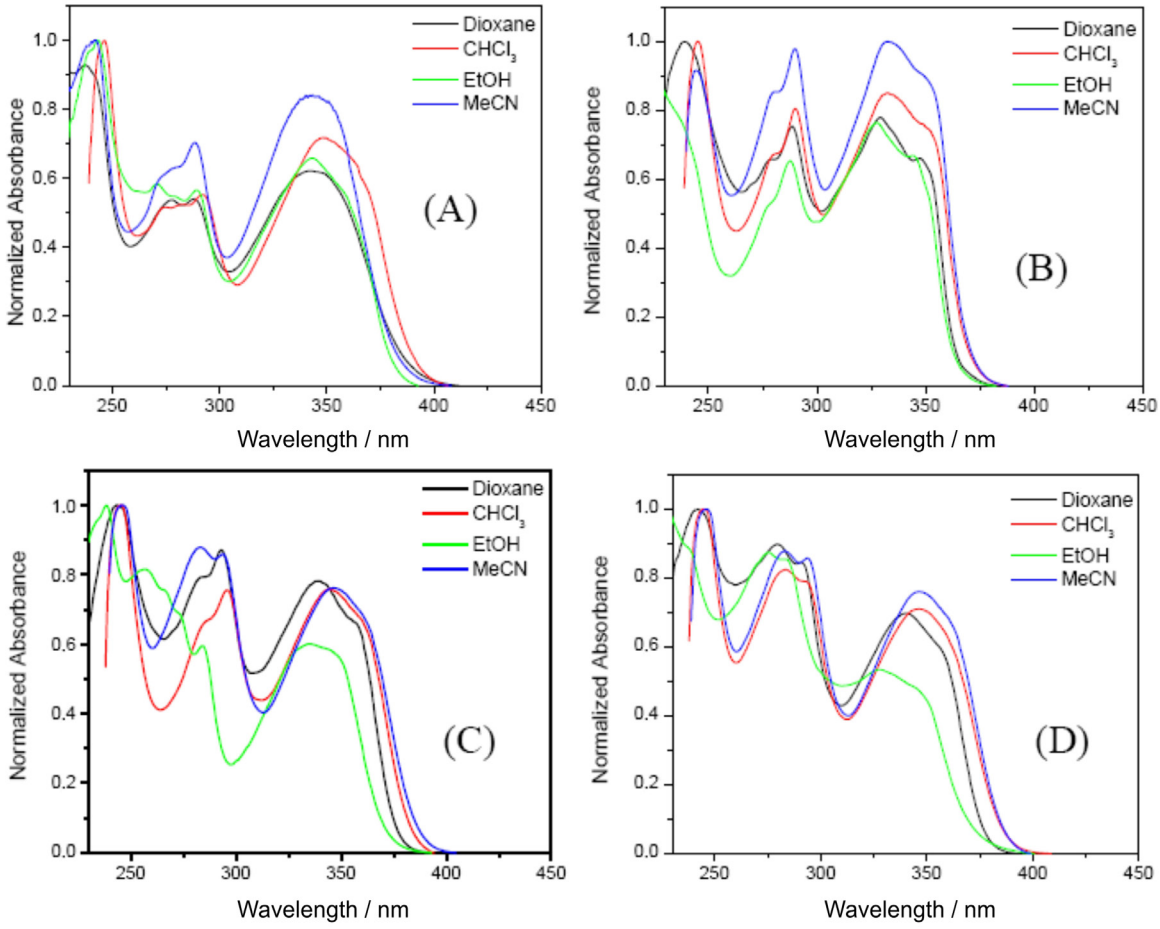

Figure 5. Absorption spectra recorded in different solvents. Compounds: (A) aldehyde **3**, (B) oxime **4**, (C) esters **6c** and (D) **8**.

Table 2. Absorption and emission data of compounds **3**, **4**, **6c** and **8** in different solvents and in the solid-state (S-s)

Entry	Solvent	Absorption peaks / nm	λ_{em} [a] / nm	Stokes' shift / nm	ϕ [b]
3	Dioxane	243.5, 289.0, 343.5	384.4	40.9	0.20
	$CHCl_3$	246.5, 292.0, 349.5	440.6	91.1	0.11
	MeCN	242.0, 288.0, 343.4	441.6	93.7	0.17
	EtOH	237.0, 288.5, 342.0	423.6	98.2	
	S-s[c]	403.8	466.8	63.0	-
4	Dioxane	239.0, 288.5, 329.5	380.2	50.7	0.30
	$CHCl_3$	245.5, 290.5, 333.0	398.0	65.0	0.29
	MeCN	244.5, 290.0, 332.2	397.6	65.4	0.21
	EtOH	221.0, 287.5, 327.5	417.0	89.5	0.25
	S-s[c]	396.8	446.0	49.2	-
6c	Dioxane	243.5, 293.5, 339.5	398.8	59.3	0.70
	$CHCl_3$	245.5, 296.0, 344.0	418.4	74.4	0.10
	MeCN	238.5, 284.0, 341.5	412.8	71.3	0.27
	EtOH	246.6, 294.0, 346.5	434.6	88.1	0.25
	S-s[c]	353.4	436.6	83.2	-
8	Dioxane	242.0, 291.0, 340.0	405.6	65.6	0.47
	$CHCl_3$	245.0, 289.0, 346.5	412.2	65.7	0.17
	MeCN	246.5, 294.0, 346.5	409.0	62.5	0.18
	EtOH	285.0, 345.0	418.8	73.8	0.40
	S-s[c]	373.8	432.2	58.4	

[a]λ_{ex} = 343 nm. [b]Relative to quinine sulfate in 0.1 mol L^{-1} H_2SO_4 as a standard (λ_{ex} = 343 nm, ϕ = 0.55). [c]Solid-state.

which is solvent dependent. In the solid state the spectra are red-shifted and show some vibrational fine structure for isoxazoline **8**. The bands at 410 and 455 nm (Figure S44 (D)) are assigned as solid-state bands and belong to crystal packing absent in solution.

Quantum yields have been measured in all solvents relative to quinine sulfate showing that efficiency is comparable to this standard.[47] As expected, the quantum yields of the esters **6c** and **8** were significantly larger than the analogous aldehyde **3** and oxime **4**. The ϕ of ester **6c** (70%) is very high in dioxane. The photostability of these compounds was determined using the protocol established by Cho *et al.*[48] The control experiments were performed using a $CHCl_3$ solution of ester **6c**. The mixture was monitorated at 296 nm and 343 nm during six months maintaning the sample at 0 °C in a amber bottle. After this period, solution of **6c** became unstable as seen clearly by the changes in the UV-Vis absorption spectra of these compound in different period of the time (Figure S45) which indicates that side reactions such as hydrolysis can occur. This photochemical behaviour was found for all the esters **6a-d** and **8**.

Conclusions

A novel series of aryl ethynylbenzaldehyde *O*-benzoyloximes **6a-d** and **8** was synthesized and their LC and photophysical were evaluated. The heat-induced decomposition of these arylaldoxime esters was observed above the clearing temperature. The mesomorphic behaviour was analysed from the first heating run, and it is nearly impossible to determine the mesophase type after first heating because the composition is presumably changed during the acquisition of the data. The thermal decomposition was also analysed using IR data. The stability of these compounds was also checked by measuring the decrease in absorption of the *O*-benzoyloximes at 230-340 nm. For aryloxime esters **6a-d**, the smectic C and nematic phase were observed during the first heating. The ester **8** exhibits the SmX mesophase. The heat-induced decomposition of these compounds probably produces the correspondent nitriles as evidenced by IR spectra. In this sense, compound **10** was prepared and compared with the mixture produced during the heat-induced aging.

Acknowledgments

This work was supported by MCT/CNPq Universal n. 471194/2008-5, PROCAD-CAPES, INCT-Catálise. B. C. A. is an undergraduate student and thanks to CNPq-PIBIC-UFRGS for her fellowship. We acknowledge FAPESC and Laboratório de Difração de Raios-X (LDRX-DF/UFSC) for the X-ray diffraction experiments.

Supplementary Information

Supplementary information (spectra data and spectra of synthesized compounds) is available free of charge at http://jbcs.sbq.org.br as PDF file.

References

1. Mayer, P.; Potgieter, K. C.; Gerber, T. I. A.; *Polyhedron* **2010**, *29*, 1423.
2. Handa, S.; Gnanadesikan, V.; Matsunaga S.; Shibasaki, M.; *J. Am. Chem. Soc.* **2010**, *132*, 4925.
3. Doronin, S. Y.; Zadymova, N. M.; Poteshnova, V.; Chernova, R. K.; Burgomistrova, A. A.; Yurasov, N. A.; *J. Anal. Chem.* **2010**, *65*, 48.
4. Filipczak, K.; Karolczak J.; Ziólek, M.; *Photochem. Photobiol. Sci.* **2009**, *8*, 1603.
5. Vorländer, D.; *Z. Phys. Chem.* **1923**, *105*, 211.
6. Kelker H.; Scheurle, B.; *Angew. Chem., Int. Ed.* **1969**, *8*, 884.
7. Criswell, T. R.; Klanderman, B. H.; Batesky, D. C.; *Mol. Cryst. Liq. Cryst.* **1973**, *22*, 211.
8. Pizzala, H.; Carles, M.; Stone, W. E. E.; Thevand, A.; *J. Chem. Soc., Perkin Trans. 2* **2000**, *5*, 935.
9. Parra, M.; Vergara, J.; Hidalgo, P.; Barberá, J.; Sierra, T.; *Liq. Cryst*. **2006**, *23*, 739.
10. Meyer, R. B.; Lièbert, L.; Strzelecki, L.; Keller, K.; *J. Physique Lett.* **1977**, *36*, L69.
11. Merlo, A. A.; Gallardo, H.; Taylor, T. R.; *Quim. Nova* **2001**, *24*, 354; Merlo, A. A.; Livotto, P. R.; Gallardo, H.; Taylor, T. R.; *Mol. Cryst. Liq. Cryst.* **1998**, *309*, 111.
12. Li, Z.; Miao, X.; Xin, H.; Deng, W.; *Mater. Chem. Phys*. **2010**, *124*, 1105.
13. Mahajan, R.; Nandedkar, H.; *Liq. Cryst*. **1998**, *24*, 173; Abraham, M. H.; Gil-Lostes, J.; Cometto-Muniz, J. E.; Cain, W. S.; Poole, C. F.; Atapattu, S. N.; Abraham, R. J.; Leonard, P.; *New J. Chem*. **2009**, *33*, 76; Wood, P. A.; Forgan, R. S.; Lennie, A. R.; Parsons, S.; Pidcock, E.; Tasker, P. A.; Warren, J. E.; *CrystEngComm* **2008**, *10*, 239; de Murillas, D. L.; Pinol, R.; Ros, M. B.; Serrano, J. L.; Sierra T.; de la Fuente, M. R.; *J. Mater. Chem.* **2004**, ***14***, 1117; Kitahara, K.; Toma, T.; Shimokawa J.; Fukuyama, T.; *Org. Lett*. **2008**, *10*, 2259; Weissflog, W.; Wiegeleben, A.; Demus, D.; *Mater. Chem. Phys*. **1985**, *12*, 461; Matos, K. S.; Mancini, D. T.; da Cunha, E. F. F.; Kuèa, K.; França, T. C. C.; Ramalho, T. C.; *J. Braz. Chem. Soc.* **2011**, *22*, 1999.
14. Boucher, J.-L.; Delaforge, M.; Mansuy, D.; *Biochemistry* **1994**, *33*, 7811.
15. Johnson, S. M.; Petrassi, H. M.; Purkey, H. E.; Palaninathan, S. K.; Mohamedmohaideen, N. N.; Nichols, C.; Chiang, K. P.; Walkup, T.; Sacchettini, J. C.; Sharpless, K. B.; Kelly, J. W.; *Med. Chem.* **2005**, *48*, 1576; De, P.; Nonappa; Pandurangan, K.; Maitra, U.; Wailes, S.; *Org. Lett.* **2007**, *9*, 2767.
16. Bassoli, A.; Borgonovo, G.; Caimi, S.; Scaglioni, L.; Morini, G.; Moriello, A. S.; Di Marzo, V.; De Petrocellis, L.; *Bioorg. Med. Chem.* **2009**, *17*, 1636; Gamba, D.; Pisoni, D. S.; da Costa, J. S.; Petzhold, C. L.; Borges, A. C. A.; Ceschi, M. A.; *J. Braz. Chem. Soc.* **2008**, *19*, 1270; de Almeida, Q. A. R.; Pereira, M. L. O.; Coelho, R. B.; de Carvalho, E. M.; Kaiser, C. R.; Jones Jr., J.; da Silva, F. M.; *J. Braz. Chem. Soc.* **2008**, *19*, 894.
17. Shrot, S.; Markel, G.; Dushnitsky, T.; Krivoy, A.; *Neuro Toxicology* **2009**, *30*, 167; dos Santos, D. R.; de Oliveira, A. G. S.; Coelho, R. L.; Begnini, I. M.; Magnago, R. F.; da Silva, L.; *ARKIVOC* **2008**, *xvii*, 157.
18. Dubrovskiy, A. V.; Larock, R. C.; *Org. Lett.* **2010**, *12*, 1180.
19. Almeida, M. R.; Leitão, G. G.; Silva, B. V.; Barbosa, J. P.; Pinto, A. C.; *J. Braz. Chem. Soc.* **2010**, *21*, 764.
20. Alonso, D. A.; Nájera, C.; Pacheco, M. C.; *Adv. Synth. Catal*. **2002**, *344*, 172.
21. Khattab, S. N.; Subirós-Funosas, R.; El-Faham, A.; Albericio, F.; *Eur. J. Org. Chem*. **2010**, *2010*, 3275.
22. Tavares, A.; Schneider, P. H.; Merlo, A. A.; *Eur. J. Org. Chem.* **2009**, *2009*, 889.
23. Bezborodov, V.; Kauhanka, N.; Lapanik, V.; *Mol. Cryst. Liq. Cryst*. **2004**, *411*, 1145; Bezborodov, V. S.; Kauhanka, N. N.; Lapanik, V. I.; Lee, C. J.; *Liq. Cryst*. **2003**, *30*, 579; Bruce, D. C.; Heyns, K.; Vill, V.; *Liq. Cryst*. **1997**, *23*, 813.
24. Tavares, A.; Ritter, O. M. S.; Vasconcelos, U. B.; Arruda, B. C.; Schrader, A.; Schneider, P. H.; Merlo, A. A.; *Liq. Cryst*. **2010**, *37*, 159.
25. Torgova, S. I.; Petrov, M. V.; Strigazzi, A.; *Liq. Cryst*. **2001**, *28*, 1439; Braga, A. L.; Schneider, P. H.; Paixão, M. W.; Deobald, A. M.; *Tetrahedron Lett*. **2007**, *47*, 7195; Merlo, A. A.; Fernandes, M. S.; *Synth. Commun*. **2003**, *33*, 1167.
26. Wan, W.; Yang, C.; Jiang, H. Z.; Deng, H. M.; Wang J.; Hao, J.; *Liq. Cryst*. **2008**, *35*, 665; Naoum, M. M.; Saad, G. R.; Nessim, R. I.; Abdel Aziz, T. A.; Seliger, H.; *Liq. Cryst*. **1997**, *23*, 789.
27. King A. O.; Negishi, E.; *J. Org. Chem*. **1978**, *43*, 358.
28. Vasconcelos, U. B.; Merlo, A. A.; *Synthesis* **2006**, *7*, 1141; Vasconcelos, U. B.; Vilela, G. D.; Schrader, A.; Borges A. C. A.; Merlo, A. A.; *Tetrahedron* **2008**, *64*, 4619.
29. Sonogashira, K.; Tohda, Y.; Hagihara, N.; *Tetrahedron Lett.* **1975**, *16*, 4467; Chinchilla, R.; Nájera, C.; *Chem. Rev*. **2007**, *107*, 874.
30. Vasconcelos, U. B.; Braun, J. E.; Ely, F.; Gallardo, H.; Merlo, A. A.; *Liq. Cryst.* **2000**, *27*, 657; Braga, A. L.; Lüdtke, D. S.; Wessjohann, L. A.; Paixão, M. W.; Schneider, P. H.; *J. Mol. Catal. A: Chem.* **2005**, *229*, 47; Han, J.; Wang, F-L.; Zhang, F-Y.; Zhu, L-R.; *Liq. Cryst.* **2010**, *37*, 1521.
31. Neises, B.; Steglich, W.; *Angew. Chem., Int. Ed.* **1978**, *17*, 522.
32. Weissflog, W.; Schubert, H.; *J. Prakt. Chem.* **1976**, *318,* 785; Weissflog, W.; König, S.; Demus, D.; Vogel, L.; Schubert, H.; *J. Prakt. Chem.* **1977**, *319*, 507; Neber, P. W.; Hartung K.; Ruopp, W.;

Ber. Dtsch. Chem. Ges. **1925**, *58*, 1234; for oxime LC see Mahajan, R.; Nandedkar, H.; *Liq. Cryst*. **1998**, *24*, 173.

33. Birgeneau R. J.; Litster, J. D.; *J. Phys. Lett.* **1978**, *39*, L-399; Gou-Ping; Chang-Chien; *J. Polym. Sci., Part A: Polym. Chem.* **1998**, *36*, 2849.
34. Hill, J. H. M.; Schmookler, L. D.; *J. Org. Chem.* **1967**, *32*, 4025; Cho, B. R.; Chung, H. S.; Cho, N. S.; *J. Org. Chem.* **1998**, *63*, 4685.
35. We have synthesized **10** using the Sonogashira protocol reacting **1** and **9** in 89% yield. The mesomorphic behaviour of **10** was analysed by DSC: *on heating* **Cr** 95.2 **N** 157.5 **I**; *on cooling* **I** 154.9 **N** 61.2 **Cr**. For related compounds, see: Hsu, H.-F.; Lin, W.-C.; Lai Y.-H.; Lin, S.-Y.; *Liq. Cryst.* **2003**, *30,* 939; Hird, M.; Toyne, K. J.; *Liq. Cryst.* **1993**, *14*, 741; Wong, M. S.; Nicoud, J.-F.; *J. Chem. Soc., Chem. Commun*. **1994**, 249.
36. Gimeno, N.; Ros, M. B.; De la Fuente, M. R.; Serrano, J. L.; *Chem. Mater.* **2008**, *20,*1262; Apreutesei, D.; Mehl, G. H.; *J. Mater. Chem*. **2007**, *17*, 4711.
37. The LC textures are typical according to the reference: Gray, G. W.; Goodby, J. W.; *Smectic Liquid Crystals: Textures and Structures*, Leonard Hill: Glasgow and London, 1984; Dierking, I.; *Texture of Liquid Crystals*, Wiley-VHC: Weinheim, 2003; Demus, D.; Richter, L.; *Texture of Liquid Crystals*, VEB Deutecher Verlag: Leipzig, 1978; Li, L.; Jones, C. D.; Magolan J.; Lemieux, R. P.; *J. Mater. Chem.* **2007**, *17*, 2313; Ayub, K.; Moran, M.; Lazar, C.; Lemieux, R. P.; *J. Mater. Chem.* **2010**, *20*, 6655.
38. Pyżuk, W.; Krówczynsk, A.; Górecka, E.; *Mol. Cryst. Liq. Cryst.* **1993**, *237*, 75; Shimizu, Y.; Oikawa, K.; Nakayama K.; Guillon, D.; *J. Mater. Chem*. **2007**, *17*, 4223; Gallardo, H.; Bryk, F. R.; Vieira, A. A.; Frizon, T. E.; Conte, G.; Souza, B. S.; Eccher J.; Bechtold, I. H.; *Liq. Cryst*. **2009**, *36*, 839.
39. Frisch, M. J.; Trucks, G. W.; Schlegel, H. B.; Scuseria, G. E.; Robb, M. A.; Cheeseman, J. R.; Zakrzewski, V. G.; Montgomery Jr., J. A.; Stratmann, R. E.; Burant, J. C.; Dapprich, S.; Millam, J. M.; Daniels, A. D.; Kudin, K. N.; Strain, M. C.; Farkas, O.; Tomasi, J.; Barone, V.; Cossi, M.; Cammi, R.; Mennucci, B.; Pomelli, C.; Adamo, C.; Clifford, S.; Ochterski, J.; Petersson, G. A.; Ayala, P. Y.; Cui, Q.; Morokuma, K.; Malick, D. K.; Rabuck, A. D.; Raghavachari, K.; Foresman, J. B.; Cioslowski, J.; Ortiz, J. V.; Baboul, A. G.; Stefanov, B. B.; Liu, G.; Liashenko, A.; Piskorz, P.; Komaromi, I.; Gomperts, R.; Martin, R. L.; Fox, D. J.; Keith, T.; Al-Laham, M. A.; Peng, C. Y.; Nanayakkara, A.; Challacombe, M.; Gill, P. M. W.; Johnson, B.; Chen, W.; Wong, M. W.; Andres, J. L.; Gonzalez, C.; Head-Gordon, M.; Replogle, E. S.; Pople, J. A.; *Gaussian, Inc*., Pittsburgh PA, 1998.
40. Altinbas, O.; Dondas, H. A.; Arslan, H.; Külcü, N.; Killner, C.; *Z. Kristallogr.* **2004**, *219*, 379.
41. Tavares, A.; Livotto, P. R.; Gonçalves, P. F. B.; Merlo, A. A.; *J. Braz. Chem. Soc.* **2009**, *20*, 1742.
42. Belmar, J.; Parra, M.; Zuñiga, C.; Fuentes, G.; Marcos, M.; Serrano, J. L.; *Liq. Cryst*. **1999**, *26*, 9.
43. Marsh, N. D.; Mikolajczak, C. J.; Wornat, M. J.; *Spectrochim. Acta*, *Part A* **2000**, *56*, 1499.
44. Cataldo, F.; *Polym. Degrad. Stab.* **2004**, *83*, 59.
45. Thomas, R.; Lakshmi, S.; Pati, S. K.; Kulkarni, G. U.; *J. Phys. Chem. B* **2006**, *110*, 24674.
46. A recent report of a series of photophysical measurements of the parent species 6-methoxy-naphthalene-2-ethynylbenzaldehyde: Guo, H.-M.; Tanaka, F. J.; *J. Org. Chem.* **2009**, *72*, 2417.
47. Keddie, D. J.; Fairfull-S, K. E.; Bottle, S. E.; *Org. Biomol. Chem*. **2008**, *6*, 3135.
48. Cho, B. R.; Kim, K. D.; Lee, J. C.; Cho, N. S.; *J. Am. Chem. Soc.* **1988**, *10*, 6145.

Submitted: October 19, 2011
Published online: April 17, 2012